Biochimica et Biophysica Acta

BBA

Gene Regulatory Mechanisms

(This is a sample cover image for this issue. The actual cover is not yet available at this time.)

The bZIP repressor proteins, c-Jun dimerization protein 2 and activating transcription factor 3, recruit multiple HDAC members to the ATF3 promoter

Ilona Darlyuk-Saadon [a], Keren Weidenfeld-Baranboim [a], Kazunari K. Yokoyama [b], Tsonwin Hai [c], Ami Aronheim [a,*]

[a] Department of Molecular Genetics, The Rappaport Family Institute for Research in the Medical Sciences, Technion-Israel Institute of Technology, 7th Efron St. Bat-Galim, Haifa 31096, Israel
[b] Graduate School of Medicine, Kaohsiung Medical University, 807 Kaohsiung City, Taiwan
[c] Department of Molecular and Cellular Biochemistry, Center for Molecular Neurobiology, Ohio State University, Columbus, OH 43210, USA

ARTICLE INFO

ABSTRACT

JDP2, is a basic leucine zipper (bZIP) protein displaying a high degree of homology with the stress inducible transcription factor, ATF3. Both proteins bind to cAMP and TPA response elements and repress transcription by multiple mechanisms. Histone deacetylases (HDACs) play a key role in gene inactivation by deacetylating lysine residues on histones. Here we describe the association of JDP2 and ATF3 with HDACs 1, 2–6 and 10. Association of HDAC3 and HDAC6 with JDP2 and ATF3 occurs via direct protein–protein interactions. Only part of the N-terminal bZIP motif of JDP2 and ATF3 basic domain is necessary and sufficient for the interaction with HDACs in a manner that is independent of coiled-coil dimerization. Class I HDACs associate with the bZIP repressors via the DAC conserved domain whereas the Class IIb HDAC6 associates through its C-terminal unique binder of ubiquitin Zn finger domain. Both JDP2 and ATF3 are known to bind and repress the ATF3 promoter. MEF cells treated with histone deacetylase inhibitor, trichostatin A (TSA) display enhanced ATF3 transcription. ATF3 enhanced transcription is significantly reduced in MEF cells lacking both ATF3 and JDP2. Collectively, we propose that the recruitment of multiple HDAC members to JDP2 and ATF3 is part of their transcription repression mechanism.

© 2012 Elsevier B.V. All rights reserved.

1. Introduction

The c-Jun dimerization protein 2 (JDP2) is a basic leucine zipper protein member of the AP-1 superfamily of transcription factors [1]. JDP2 is constitutively expressed in all tissues and cell lines tested [2]. The bZIP domain of JDP2 shares a high degree of homology with the activating transcription factor 3 (ATF3) protein [2]. ATF3 is an immediate early gene that is highly induced in response to multiple cell stresses [3,4].

Depending on its dimerization partner, target promoter and cellular context, ATF3 can either act as a transcriptional activator or repressor [5,6]. Under certain circumstances, both JDP2 and ATF3 can activate transcription. ATF3 and JDP2 can potentiate transcription following hetero-dimerization with Chop10 [7] and ATF3 can also activate transcription following interaction with c-Jun [5]. JDP2 was described as a co-activator of transcription with various members of the steroid hormone receptor family [8].

Nevertheless, both ATF3 and JDP2 are still considered as bZIP transcription repressor proteins. JDP2 suppresses transcription by multiple mechanisms that involve competition on AP-1 DNA sequences [2,9], interfering with AP-1 complexes and competing with JNK phosphorylation [10,11].

JDP2 was found to directly bind histones, inhibiting their acetylation by the p300 protein [12]. Moreover, JDP2 was suggested to have nucleosome assembly activity resulting in chromatin condensation and a transcription repressive state [12]. Subsequently, it was demonstrated that JDP2 can indirectly recruit histone deacetylase 3 (HDAC3) to the c-Jun promoter [13].

JDP2 and ATF3 were shown to regulate the expression of numerous genes involved in multiple biological processes including differentiation, proliferation, inflammation and apoptosis [1,14]. Interestingly, ATF3 and JDP2 bind to the ATF3 proximal promoter and repress ATF3 transcription [15,16]. Both JDP2 and ATF3 play a dichotomous role in cell differentiation processes [13,17] and in carcinogenesis [18–20]

depending on the cellular context. Here we describe the isolation of multiple HDACs as possible protein partners for both JDP2 and ATF3 and their potential role in the regulation of gene transcription.

2. Materials and methods

2.1. Antibodies and reagents

Trichostatin A (TSA) was purchased from Sigma-Aldrich Ltd. (T1952). The primary monoclonal antibodies used: anti-Myc (9E10, Babco Inc.), anti-HA (12CA5, Babco Inc.), anti-phospho-c-Jun (SC-822, Santa-Cruz), anti-Flag M2 (F1804) and anti-α-tubulin (T9026) were from Sigma-Aldrich Ltd. The primary polyclonal antibodies used: anti-HDAC3 (H3034, Sigma-Aldrich Ltd.), anti-MBP (SC-808), anti-GAPDH (SC-25778), anti-HDAC1 (SC-7872) and anti-HDAC2 (SC-7899) were from Santa-Cruz, anti-JDP2 and anti-ATF3 were prepared in our laboratory. Anti-Flag and anti-MBP antibodies were used at a dilution of 1:1000 and anti-α-tubulin 1:2000. All other antibodies were used at a dilution of 1:500. For ChIP analysis anti-acetyl-histone H4 (06-866) from Upstate technologies was used.

2.2. Plasmids used in this study

pCS2 + MT-HDAC6-Flag expression plasmid encoding the full length human HDAC6 was kindly provided by Dr. S. Hook (Fred Hutchinson Cancer Research Center, Seattle, USA). pcDNA3.1-HDAC1-Flag, pcDNA3.1-HDAC3-Flag and pcDNA3.1-HDAC4-Flag expression plasmids encoding the human HDAC1 (13820), HDAC3 (13819) and HDAC4 (13821) were obtained from the Addgene organization [21]. pCS2 + MT-HDAC5 expression plasmid expressing the human HDAC5 was kindly provided by Dr. A. Orian (Technion, Israel). The pCS2 + MT plasmid was used to express human HDAC10.

The mammalian expression vector pCEFL was used to express the full length and all HA-tagged rat JDP2 deletion constructs. The following constructs were used: HA-JDP2 1–123 (a.a. 1–123), HA-JDP2 1–110 (a.a. 1–110) and HA-JDP2 1–94 (a.a. 1–94). HA-tagged human full length and ATF3 constructs 1–137 (a.a. 1–137) and 1–108 (a.a. 1–108) were expressed using the pcDNA-3XHA mammalian expression plasmid. The pcDNA3.1-Flag plasmid was used to express the HDAC1 and HDAC3 C terminal truncated constructs (a.a. 1–318 and 1–314, respectively).

His-tagged JDP2 and ATF3 were expressed using the bacterial expression plasmids pET and pQE-80L, respectively. The bacterial expression plasmid pMAL-p4X (NEB) was used to express the maltose binding protein (MBP) fused to the human HDAC6-C fragment (MBP-HDAC6-C) and the full length HDAC3 (MBP-HDAC3). The bacterial expression plasmid pMAL-p5X (NEB) was used to express MBP that was used as a control for the *in vitro* binding assays.

Yeast expression plasmids Met-Myc-Ras-Pak, Met-Myc-Ras-JDP2 BZ and Met-Myc-Ras-ATF3 were used as previously described [7]. The pMyr empty expression plasmid and pMyr-HeLa cDNA library were purchased from Stratagene Inc. All constructed plasmids were verified by DNA sequencing.

2.3. Ras recruitment system and yeast manipulation

Conventional yeast transfection and manipulations were performed as previously described [7,22]. Briefly, transformants were selected and grown on glucose containing plates lacking either uracil or leucine and incubated at 24 °C. Subsequently, colonies were replica plated onto galactose plates lacking methionine to induce the expression of the prey and bait proteins. Plates were incubated at 36 °C to test for Ras-bait membrane translocation and complementation of the Cdc25-2 temperature-sensitive phenotype.

2.4. Cell culture and transient transfections

Mouse embryo fibroblast (MEF) cell lines were generated as previously described [23]. The establishment of MEFs received the approval of the Technion Committee for the Supervision of Animal Experiments (application # IL-129-12-2008).

C57/Bl6 JDP2KO [24] and C57/Bl6 ATF3KO [25] mice were crossed to generate mice harboring disruption for both the alleles. MEF cell lines were generated from C57/Bl6 wild type mice (WT) and JDP2–ATF3 double knockout mice (DKO).

Human embryonic kidney 293T (HEK-293T), human lung carcinoma (H1299) [26], mouse sertoli cells (TM4) [27] and MEF cell lines were maintained in Dulbecco's modified Eagle's medium (DMEM) containing 10% FCS, 100 u/ml penicillin and 0.1 μg/ml streptomycin and grown at 37 °C and 5% CO_2.

HEK-293T cells were transfected with the appropriate expression plasmid using the calcium-phosphate (Ca_2PO_4) method [28]. A day before the transfection 1×10^6 cells were seeded on 100 mm plate. The total amount of plasmid DNA was adjusted to 10–12 μg in a total volume of 1000 μl. Cells were replaced with fresh medium 4–5 h post transfection and harvested 24 h post transfection.

MEF cells were transfected using the JetPRIME DNA Transfection Reagent (PolyPlus transfection Inc., Cat# 114-01) according to the manufacturer's instructions.

For RNA extractions, 7×10^5 MEF cells/100 mm plate were seeded a day before the extraction and treated as described.

Serum induction: MEF cells were serum starved (0.1% FCS) for 16–18 h followed by 20% FCS stimulation 4 h prior to cell extraction. Where indicated, 100 nM TSA was added to serum starved cells together with serum stimulation.

2.5. Western blot analysis

Cells were lysed in whole cell extraction buffer (WCE) containing: 25 mM HEPES pH 7.7, 0.3 M NaCl, 1.5 mM $MgCl_2$, 0.2 mM EDTA, 0.1% Triton X-100, 0.5 mM DTT, 20 mM β-glycerolphosphate, 0.1 mM Na_2VO_4, 100 μg/ml PMSF and protease inhibitor cocktail 1:100 (Sigma Aldrich, #P8340). SDS-sample buffer was added to the extracts followed by a 5 min boiling. The proteins were then separated on a 10% or 12% SDS-PAGE, and then transferred to a nitrocellulose membrane. Blots were blocked in 5% nonfat dry milk in PBS and washed three times in PBS after the incubation with the corresponding primary and secondary antibodies. Proteins were detected using the corresponding HRP-conjugated secondary antibodies obtained from Sigma-Aldrich (anti-rabbit Cat# A0545, anti-mouse Cat# A0168) and Jackson (anti-mouse light chain Cat# 115-035-174, anti-rabbit light chain Cat# 211-032-171). Nuclear extract fractionation was performed as previously described [29].

2.6. Immunoprecipitation

Protein extracts (400–600 μg in WCE buffer) were pre-cleared with species matched non-relevant antibodies. The lysates were then incubated with antibodies against Myc, Flag, JDP2 or ATF3 overnight at 4 °C. Protein-A sepharose beads (Sigma-Aldrich, Cat# P3391) were then added to the lysates and incubated for 1 h at 4 °C. Samples were washed four times with WCE buffer. The precipitated proteins were eluted using SDS-sample buffer, boiled and then processed by Western blot analysis.

2.7. In vitro protein binding assay

His-JDP2 and His-ATF3 were bacterially purified using Ni-NTA Agarose beads (Qiagen Cat#1018244) according to the manufacturer's instructions. MBP and recombinant MBP-HDAC6-C and MBP-HDAC3 proteins were purified using an amylose resin (New England Biolabs, Cat# E8021S) according to the manufacturer's instructions. His-tagged

protein (5 μg) was incubated with 10 μg MBP or MBP-tagged protein and 0.5 mg BSA for 2 h at 37 °C. The amylose resin was pre-blocked with 0.5 mg BSA for 1 h at 4 °C and then incubated with the indicated pre-incubated protein complexes for 1 h at 4 °C. Following five washes with column buffer (20 mM Tris–HCl pH 7.4, 200 mM NaCl, 1 mM EDTA, 1 mM DTT), the precipitated proteins were eluted using the column buffer containing in addition 10 mM D-Maltose (Sigma-Aldrich, Cat# M5885). Following the addition of SDS-sample buffer, the samples were boiled and then processed by Western blot analysis.

2.8. mRNA preparations

mRNA was purified from MEF cells using High Pure RNA Isolation Kit (Roche Cat# 11828665001) according to the manufacturer's protocol.

2.9. Real time PCR

cDNA was synthesized using a High Capacity cDNA Reverse Transcription kit (AB Applied Biosystems Cat# 4368814) according to the manufacturer's instructions. 1 μg of RNA was used for each sample. qRT-PCR was conducted using the Rotor-Gene Q (Qiagen Inc.) equipment with the absolute blue SYBR green ROX mix (Thermo scientific Cat# AB4162/B).

Primers corresponding to the mouse genes used were:

Name of gene	Forward 5′–3′	Reverse 5′–3′
ATF3	GCTGCTGCCAAGTGTCGAAA	CGGTGCAGGTTGAGCATGTA
Chop	GGGCCAACAGAGGTCACAC	CTTCATGCGTTGCTTCCCA
c-Jun	CCTTCTACGACGATGCCCTC	GGTTCAAGGTCATGCTCTGTTT
β2m	TTCTGGTGCTTGTCTCACTGA	CAGTATGTTCGGCTTCCCATTC
GAPDH	TTGCCATCAACGACCCCTTCAT	AGACTCCACGACATACTCAGCA

2.10. Chromatin immunoprecipitation (ChIP)

ChIP was performed using a ChIP assay kit (Cat #17-295, Upstate technologies) according to the manufacturer's instructions. In principle, cells were cross-linked by formaldehyde and the DNA was sonicated to produce 500–1000 bp DNA fragments using a Bioruptor (Diagnode Inc.). 5 μl of anti-acetylated histone 4 antibody was used for immunoprecipitation followed by extensive washes. The cross-link was reversed and the DNA was purified. Subsequently, qRT-PCR was used to assess the presence of DNA fragments derived from the mouse ATF3 promoter.

Oligonucleotides used in qRT-PCR were:

Name of fragment	Forward 5′–3′	Reverse 5′–3′
−1538 −1388	GCTCAGACCCTCGGAATTAC	GTACTCAAATCTGGTGGCGG
−1134 −1262	CCTTTCCTCAGGACCGTAAC	GTAAAGACAGAGGCACCTGC
−1023 −874	TTTCCTGATATCCAGGCGGA	GAGGAAAGATTTGGAGAGATC
−679 −540	TGCCGAATGTCTACGTTAACC	AAGGGATAGCGGTGACAATC
−410 −268	AACCTAGCGGAGGGAGAGAT	TCTATCTCCTTATCAGGCTGG
−105 to +15	ATTACGTCAGCCTGGGATTG	TCTCGCTGAGTGAGACTGTG

2.11. Statistical analysis

Statistical analysis was performed using the Student's unpaired t test with a two-tailed distribution.

3. Results

3.1. RRS screening and isolation of HDAC6 as a JDP2 and ATF3 interacting protein

JDP2 and ATF3 proteins (termed herein bZIP repressors) share an 89% homology within their bZIP domains, however, significantly

lower homology is observed in regions outside of this domain [30]. In an attempt to identify common proteins that bind to the bZIP repressor proteins, we used the Ras recruitment system (RRS) [31,32]. The RRS system is a modified two-hybrid approach in which protein–protein interactions occur within the cytoplasm of a CDC25-2 yeast temperature sensitive strain [22]. Following a *bona fide* protein–protein interaction, cytoplasmic Ras is recruited to the plasma membrane resulting in the complementation of the yeast Ras viability pathway. CDC25-2 yeast strain viability is easily monitored at the restrictive temperature of 36 °C [31,32]. Two baits corresponding to either the JDP2 bZIP domain (JDP2-BZ a.a. 74–135) or the full length ATF3 (ATF3 a.a. 1–181) (Fig. 1A constructs ii and iii, respectively) were used independently to screen a HeLa myristoylated cDNA expression library as previously described [7]. DNA sequence analysis of multiple candidate clones revealed the isolation of the C-terminal domain of a Class II HDAC protein, HDAC6 (Fig. 1A construct v) [33]. Since HDAC6 was isolated numerous times with both JDP2 and ATF3 baits, we sought to further characterize the association between the bZIP repressor proteins and HDAC proteins. The HDAC family is subdivided into three main subfamilies according to homologies to the yeast HDAC prototype [34]. Class I HDACs are mainly nuclear while Class II HDACs display both nuclear and cytoplasmic localization. Class III HDACs, the Sirtuin, contain a conserved catalytic domain with low homology to the Class I and II HDACs. In addition, members of the Class III HDAC require NAD as a substrate [35,36]. HDAC6 belongs to Class IIb consisting of two functional HDAC catalytic domains. Cellular fractionation of human and mouse cell lines demonstrated that endogenous HDAC6 protein is present in both cytoplasmic and nuclear fractions (Supplementary Fig. 1A). The mouse HDAC6 protein is shorter than the human counterpart by 66 residues thus migrates faster on SDS-PAGE. However, HDAC6 is present at even higher levels in the nucleus. α-Tubulin and JDP2 are solely detectable in the cytoplasmic and nuclear fraction respectively, thus signifying the fractionation quality. Therefore, HDAC6 can potentially interact with the nuclear localized bZIP repressors.

To confirm the interaction between the bZIP repressor proteins and HDAC6 in yeast, we co-transfected CDC25-2 cells with plasmids encoding the original baits (JDP2-BZ or ATF3) together with the HDAC6 prey plasmid (Fig. 1A–B). The HDAC6 prey plasmid encodes for the C-terminal 131 a.a. (Fig. 1A construct v). Yeast cells expressing the HDAC6 prey peptide with both of the bZIP repressor baits were able to grow at the restrictive temperature (Fig. 1B). Cell growth was comparable to the growth of yeast cells expressing *bona fide* protein pairs encoding for the p21 activating kinase (Ras-PAK) and CDC42 homologous protein (Myr-Chp) [37]. The JDP2 bait that associated with the HDAC6 C-terminal peptide corresponded to 62 a.a. that included the JDP2 bZIP domain (Fig. 1A–B).
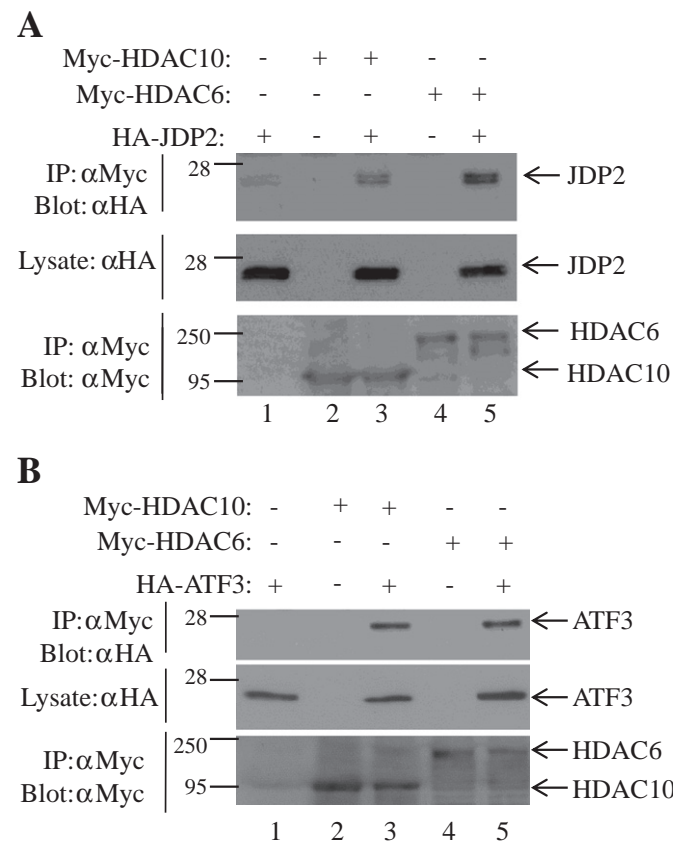
3.2. bZIP repressor proteins associate with two members of the Class IIb HDACs in mammalian cells

We next sought to confirm the interaction between the bZIP repressor proteins and full length HDAC6 protein in mammalian cells. Human embryonic kidney 293 (HEK-293T) cells were transfected with expression plasmids encoding HA-tagged-JDP2 or HA-tagged-ATF3 together with full length Myc-tagged-HDAC6. HDAC6 was immunoprecipitated from cell lysates using an anti-Myc antibody, and the presence of JDP2 or ATF3 in the protein complex was detected by Western blotting using an anti-HA antibody (Fig. 2A–B). Both HA-JDP2 and HA-ATF3 were efficiently precipitated by Myc-HDAC6, confirming that the full length bZIP repressor and HDAC6 proteins interact in HEK-293T mammalian cells.

We next examined whether the bZIP repressors are also able to associate with another Class IIb member, HDAC10 [36]. Myc-tagged HDAC10 was co-expressed with either HA-JDP2 or HA-ATF3 in HEK-293T cells and the cell lysate was immunoprecipitated with anti-Myc antibody (Fig. 2A–B). Indeed, both HA-JDP2 and HA-ATF3 were
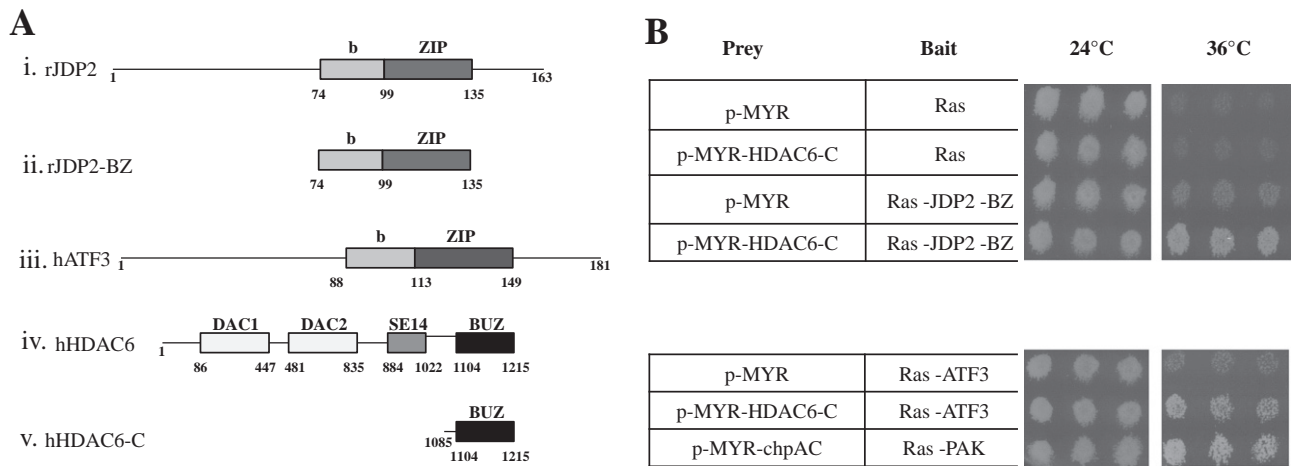
Fig. 1. Identification of the JDP2/ATF3–HDAC6 association in yeast using the RRS system. A. Schematic representation of the full length rat JDP2 (rJDP2), human ATF3 (hATF3) and human HDAC6 (hHDAC6) and their corresponding constructs used in the RRS system. Amino acid positions are numbered. The following domains are abbreviated: basic (b), leucine zipper (ZIP), deacetylase domain (DAC), Ser-Glu tetradecapeptide (SE14) and Binder of ubiquitin Zn finger domain (BUZ). B. Yeast transformants expressing the indicated prey and bait proteins were grown at 24 °C for 2 days and subsequently were replica plated onto galactose plates lacking methionine, leucine and uracil, and grown at 36 °C and 24 °C (right and left panels, respectively). The baits fused to Ras are the p21 activating kinase regulatory domain (Ras-Pak), the JDP2 basic-leucine zipper domain (Ras-JDP2-BZ) and full length ATF3 (Ras-ATF3). An empty pMyr expression vector, pMyr-Chp activated mutant (pMyr-ChpAc) [37] or human HDAC6-C fused to v-Src myristoylation signal (pMyr-HDAC6-C) were used as prey proteins.
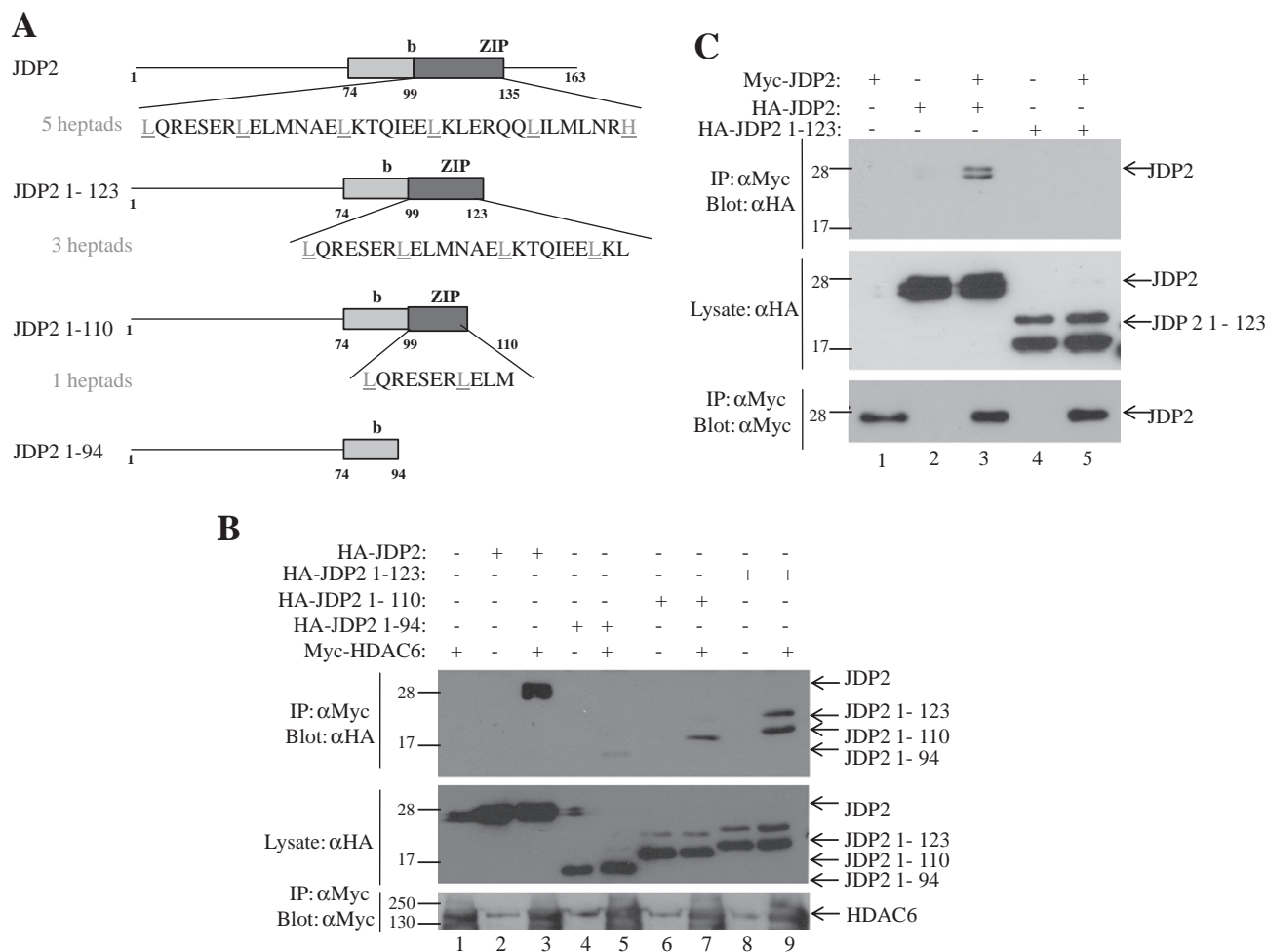
efficiently co-precipitated with Myc-HDAC10. This result suggests that bZIP repressors interact with the two members of the Class IIb HDACs.

3.3. HDAC6 association with the bZIP repressors does not require a functional leucine zipper

The JDP2 bZIP peptide that displays association with HDAC6 in yeast consists of 62 a.a. composed of a basic leucine zipper (Fig. 1A). The leucine zipper domain is composed of five heptads that form a coiled-coil structure responsible for homodimerization as well as heterodimerization with other members of the bZIP family of transcription factors [30,38] (Fig. 3A). To examine whether the bZIP repressor proteins require a functional leucine zipper motif for their association with HDAC6, we used a series of JDP2 truncated mutants in which the leucine zipper heptad motifs were removed incrementally (Fig. 3A). A co-immunoprecipitation experiment showed that Myc-HDAC6 interacted poorly with the JDP2 protein lacking the complete leucine zipper (JDP2 1–94 Fig. 3B, lane 5). Subsequently, JDP2 protein fragment containing the first leucine zipper heptad (JDP2 1–110) displayed a stronger association, JDP2 containing three leucine zipper heptads (HA-JDP2 1–123) displayed a prominent association with HDAC6 (Fig. 3B, compare lanes 7 and 9). Repeated experiments indicated that the HA-JDP2 1–123 displayed the highest association while HA-JDP2 1–94 the worst.

To determine whether JDP2 homo-dimerization is required for HDAC6 association, we co-expressed the JDP2 fragment lacking the last two heptads (HA-JDP2 1–123) with full length JDP2 (Myc-JDP2) and examined their ability to dimerize by co-immunoprecipitation. Full length JDP2 failed to interact with JDP2 1–123 (Fig. 3C, lane 5). Thus, we conclude that JDP2 homo-dimerization is not a pre-requisite for the association with HDAC6.

JDP2 and ATF3 display an 89% homology within the 62 a.a. region comprising the bZIP domain found to be necessary for the association with HDAC6. In contrast, the region located N-terminally to the basic domain displays only a 44% homology (Fig. 4A). To determine whether the minimal ATF3 domain that interacts with HDAC6 requires the nonfunctional N-terminal leucine zipper motif as well, we designed a similar set of truncation mutants in which increasing portions of the ATF3 leucine zipper domain were deleted (Fig. 4B).

Fig. 2. Validation of the HDAC6/HDAC10 and JDP2/ATF3 interaction in mammalian cells. A–B. HEK-293T cells were transfected with Myc-HDAC6 or Myc-HDAC10 and HA-JDP2 (A) or HA-ATF3 (B) in various combinations as indicated. Cell lysates were subjected to immunoprecipitation with anti-Myc antibodies followed by Western blotting with either anti-HA or anti-Myc (upper panel and lower panel, respectively). The expression level of HA-JDP2 (A) or HA-ATF3 (B) was determined by blotting 10% of total cell lysate with anti-HA antibodies (middle panels). Protein molecular weight markers (in kDa) are indicated on the left-hand side.

Fig. 3. A partial leucine zipper motif is required for the association of JDP2 with HDAC6. A. Schematic representation of the JDP2 full length and truncated C-terminal constructs used in the experiments. Underlined gray amino acids represent the heptad leucine zipper residues. B. HEK-293T cells were transfected with Myc-HDAC6, the full length HA-JDP2 and different HA-JDP2 fragments in various combinations as indicated. Cell lysates were subjected to immunoprecipitation with anti-Myc antibodies followed by Western blotting with either anti-HA or anti-Myc (upper panel and lower panel, respectively). The expression level of the full length HA-JDP2 and HA-JDP2 constructs was determined by blotting 10% of total cell lysate with anti-HA antibodies (middle panel). C. HEK-293 T cells were transfected and cell lysates were treated as indicated in B. The expression level of the full length HA-JDP2 and HA-JDP2 1–123 construct was determined by blotting 10% of total cell lysate with anti-HA antibodies (middle panel). Protein molecular weight markers (in kDa) are indicated on the left-hand side.

Co-immunoprecipitation analysis clearly demonstrated that the three leucine zipper heptads located N-terminally within ATF3 were not necessary for the association with HDAC6, since an ATF3 fragment lacking the complete leucine zipper domain interacted with HDAC6 as well (Fig. 4C compare lanes 5 and 7). Nevertheless, the full length ATF3 protein displayed the strongest binding to HDAC6 as compared with either ATF3 1-108 or ATF3 1-137 (Fig. 4C).

3.4. The bZIP repressor proteins associate with multiple members of Class I and II HDAC

To examine whether the bZIP repressor proteins are able to associate with other HDAC proteins, co-immunoprecipitation experiments were performed with multiple members of Class I (HDACs 1 and 3) and Class IIa (HDACs 4 and 5) [36]. Towards this end, we used the HA-tagged JDP2 and ATF3 truncated proteins encoding for a.a. 1–123 and 1–137 respectively, that were found to efficiently associate with HDAC6. Immunoprecipitation of HDACs 1, 3 and 5 resulted in co-precipitation of JDP2 (Fig. 5A–B), while HDAC4 showed modest pre-cipitation of JDP2 protein as compared with HDAC5 (Fig. 5B compare lanes 3 and 5).

Similar results were obtained with the different HDAC members and ATF3 (Fig. 5C) *i.e.* strong ATF3 precipitation with HDACs 1, 3 and 5, and a weaker interaction with HDAC4 (Fig. 5C lane 7). Repeated experiments, taking into consideration the HDAC levels (1, 3, 4, and 6 using the same Flag antibody), indicated that HDAC6 consistently displayed the strongest binding toward these bZIP repressors and HDAC4 the lowest. The strong binding of HDAC6 to the bZIP repressors may explain the repeated isolation of HDAC6 cDNA from the yeast RRS screening. Collectively, ATF3 and JDP2 interact alike with HDAC subfamilies including Class I and II members, while weaker association is observed with the Class IIa member, HDAC4.

To examine the possible interaction of endogenous JDP2 with various HDACs in cell lysates, we performed co-immunoprecipitation experiment with cell lysates derived from MEF cells using anti-JDP2 followed by a Western blotting probed with multiple anti-HDACs anti-bodies (Fig. 6A). We were able to demonstrate the interaction between HDACs 1, 2 and 3 with JDP2. The association shown with HDAC3, is consistent with previous studies that have shown the interactions between the endogenous proteins, JDP2 and HDAC3 [13]. To test the interaction with endogenous ATF3, serum starved MEF cells were treated by serum for 1 h to induce ATF3 expression. Subsequently, anti-ATF3 immunoprecipitated cell lysate was examined for the presence of
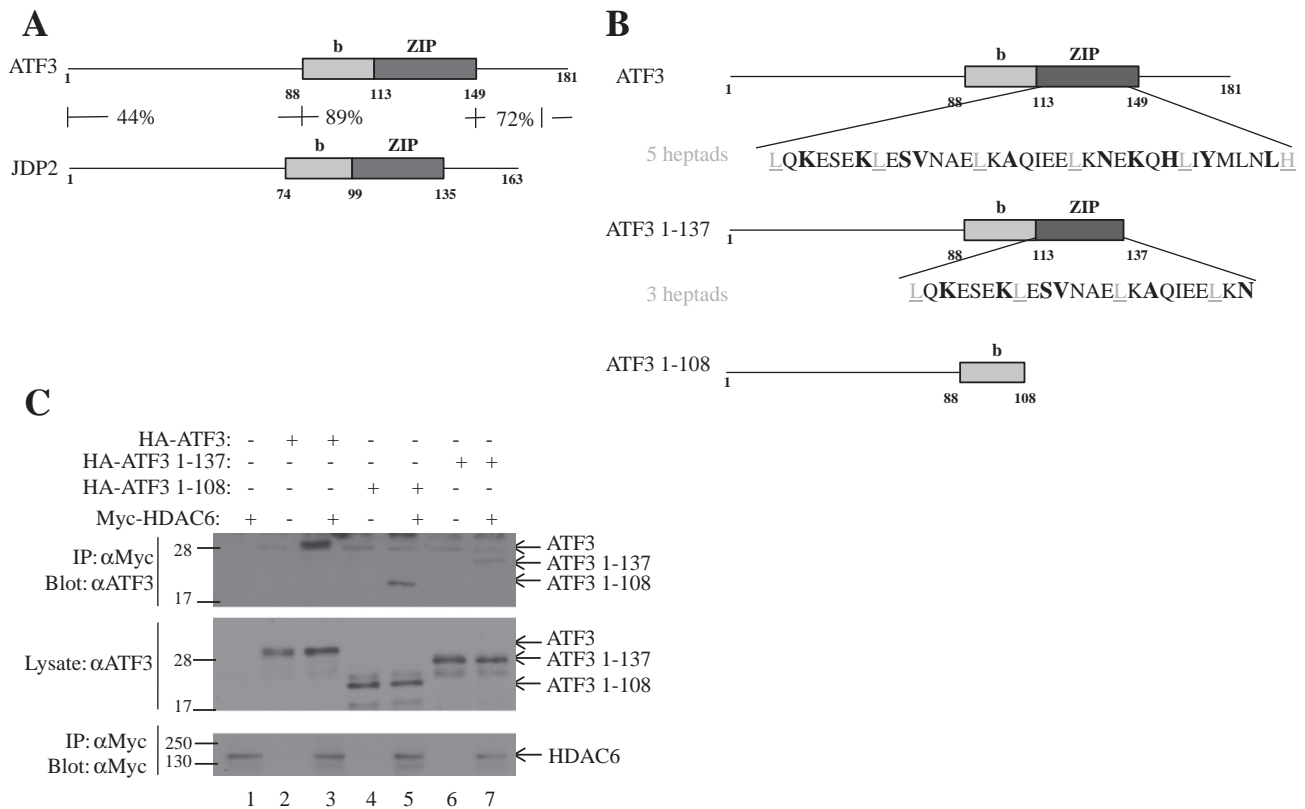
Fig. 4. The ATF3 N-terminal basic region is required for the association with HDAC6. A. Schematic representation of the percent homology between JDP2 and ATF3 proteins at the indicated domains. B. Schematic representation of the full length and the truncated C-terminal constructs of ATF3 used in the experiments. Underlined gray amino acids represent the heptad leucine zipper residues. Bold amino acids represent the amino acids that differ between ATF3 and JDP2. C. HEK-293T cells were transfected with Myc-HDAC6, the full length HA-ATF3 and HA-ATF3 deletion mutants in various combinations as indicated. Cell lysates were subjected to immunoprecipitation with anti-Myc antibodies followed by Western blotting with either anti-ATF3 or anti-Myc (upper panel and lower panels, respectively). The expression level of the full length HA-ATF3 and HA-ATF3 C-terminal deletion constructs was determined by blotting 10% of total cell lysate with anti-ATF3 antibodies (middle panel). Protein molecular weight markers (in kDa) are indicated on the left-hand side.

various HDACs by Western blotting. Indeed, ATF3 association with endogenous HDAC2 and HDAC3 but not with HDAC1 was observed (Fig. 6B). Previously, HDAC1 was shown to bind ATF3 [39]. Our inability to reproduce this result may be due to the difference in the sensitivity of the antibody used.

3.5. bZIP repressors associate with the DAC domain of Class I HDACs

Class I HDACs share an N-terminal DAC domain and differ mainly in their C-terminal region [36]. To explore the possibility that the bZIP repressors associate with this domain within the Class I family, we used HDAC1 and HDAC3 deletion mutants lacking the C-terminal non-homologous domain (Fig. 7A) and examined their interaction with JDP2 minimal binding domain corresponding to a.a. 1–123. The JDP2 fragment was efficiently precipitated by the DAC domains of HDAC1 and HDAC3 (Fig. 7B). Similar results were obtained with the ATF3 fragment corresponding to a.a 1–137 (Fig. 7C and data not shown). Thus we conclude that class I HDACs associate with the bZIP repressors *via* their DAC homology domain.

3.6. bZIP repressors interaction with HDAC 3 and HDAC 6 is direct

We next examined whether the interaction between the bZIP repressor proteins and HDACs occurs *via* a direct protein–protein interaction. Towards this end, we purified to homogeneity bacterially expressed maltose binding protein (MBP) and MBP fused to proteins corresponding to either the HDAC6-C-terminal domain (Fig. 1A construct v) or to full length HDAC3. Recombinant purified His-tagged JDP2 or ATF3 were allowed to interact with the MBP purified proteins *in vitro* followed by precipitation by amylose–sepharose beads. Following extensive washes,

the precipitated proteins were analyzed by Western blotting with either anti-JDP2 or anti-ATF3 antibodies (Fig. 8A–D, bottom panels). The MBP protein failed to associate with either His-JDP2 or His-ATF3, but MBP-HDAC3 and MBP-HDAC6-C were able to efficiently precipitate both His-JDP2 and His-ATF3 (Fig. 8A–D, lanes #3). A previous report failed to demonstrate direct interactions between *in vitro* translated JDP2 and HDAC3 [13]. Interestingly, we found that the association between HDAC3 with the bZIP repressors was highly dependent on the temperature used during the incubation period (Supplementary Fig. 2). Interactions were optimal for protein binding at 37 °C.

3.7. JDP2 and ATF3 are required to maintain ATF3 promoter transcription by HDAC recruitment

We next sought to investigate the physiological relevance of the association between the bZIP repressor proteins and the HDAC protein family. We first determined whether HDACs are involved in the inhibition of transcription of genes known to be regulated by both JDP2 and ATF3. The best characterized bZIP repressor target gene is ATF3 itself [15,16]. Towards this end, exponentially growing MEF cells were grown in the presence or absence of the potent HDAC inhibitor, TSA for 4 h, and the transcription levels of ATF3 and GAPDH were analyzed by qRT-PCR (Fig. 9A). GAPDH mRNA was used to normalize ATF3 levels, since it is not a bZIP repressor target gene nor is its expression levels altered following TSA addition. We found that ATF3 mRNA levels were significantly elevated (twelve fold) following the addition of TSA (Fig. 9A).

We sought to examine whether the potentiation of ATF3 transcription in the presence of TSA is dependent on the level of JDP2 and ATF3 in the cell. To explore this, we created a double knockout
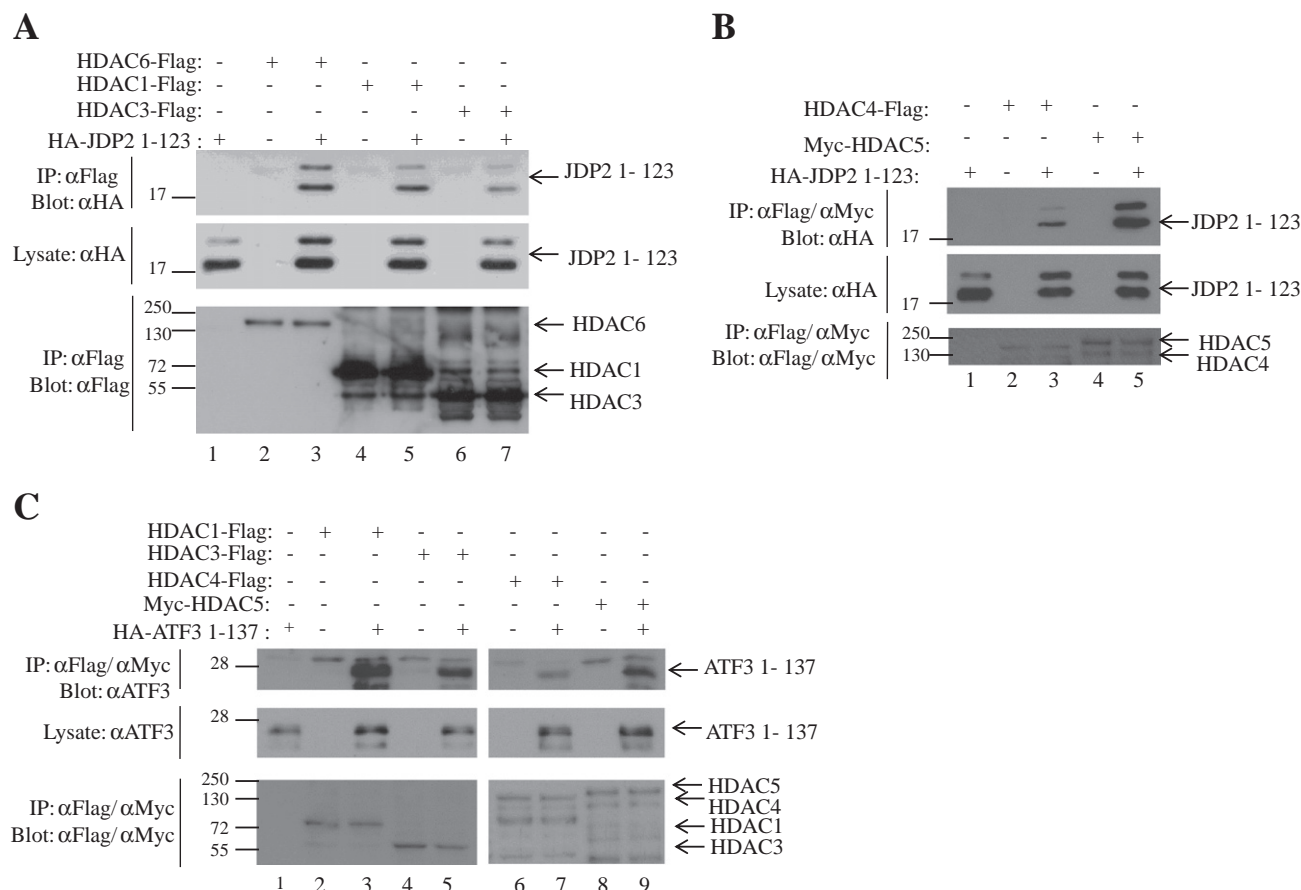
Fig. 5. JDP2 and ATF3 associate with multiple members of class I and II HDACs. A. HEK-293T cells were transfected with the HA-JDP2 1-123 construct (Fig. 3A) and flag-tagged HDACs 1, 3 and 6 in various combinations as indicated. Cell lysates were subjected to immunoprecipitation with anti-Flag antibodies followed by Western blotting with either anti-HA (upper panel) or anti-Flag (lower panel). The expression level of HA-JDP2 1–123 was determined by blotting 10% of the total cell lysate with anti-HA antibodies (middle panel). B. HEK-293T cells were transfected with the indicated plasmids and cell lysates were subjected to immunoprecipitation with anti-Flag antibodies (lanes 1–3) or with anti-Myc (lanes 4–5) followed by Western blotting with either anti-HA (upper panel) and anti-Flag or anti-Myc (lower panel). The expression level of HA-JDP2 1–123 was determined by blotting 10% of total cell lysate with anti-HA antibodies (middle panel). C. HEK-293T cells were transfected with a HA-ATF3 1–137 construct (Fig. 4B) and flag-tagged HDAC 1, 3, 4 and Myc-HDAC5 in various combinations as indicated. Cell lysates were subjected to immunoprecipitation with anti-Flag (lanes 1–7) or with anti-Myc antibodies (lanes 8–9) followed by Western blotting with anti-ATF3 (upper panel) and with either anti-Myc or anti-Flag (lower panel) antibodies. The expression level of HA-ATF3 1–137 was determined by blotting 10% of total cell lysate with anti-ATF3 antibodies (middle panel). Protein molecular weight markers (in kDa) are indicated on the left-hand side.

(DKO) mouse strain lacking both JDP2 and ATF3 by crossing ATF3KO mouse [25] with a JDP2KO mouse [24] for several generations. The DKO mice were born at the expected Mendelian ratio and displayed no overt phenotype (Darlyuk-Saadon and Aronheim unpublished results). The ATF3KO allele lacks exon 2 which prevents ATF3 protein translation but preserves ATF3 mRNA transcription. Thus, ATF3 mRNA can be analyzed by qRT-PCR with primers corresponding to exons 3 and 4 [25]. MEF cells were prepared from mice harboring double mutated alleles for both JDP2 and ATF3 (DKO) and the transcript of the above mentioned genes were analyzed by qRT-PCR in the presence and absence of TSA. DKO MEF cells displayed a significant reduced potentiation of ATF3 transcription following TSA addition (Fig. 9A). It should be noted that the ATF3 basal transcript level is significantly higher in DKO MEF cells (Supplementary Fig. 3A) which is consistent with the absence of both JDP2 and ATF3 repressor proteins [15,16]. Interestingly, two other known JDP2 target genes CHOP10 [40] and c-Jun [13] showed no significant change in their transcript level in response to TSA treatment (Fig. 9A). In exponentially growing cells, one can argue that the ATF3 protein is found below the detectable level (Supplemental Fig. 1B). To assess ATF3 contribution, we therefore performed the same assay in serum-starved MEF cells that were stimulated with serum for 4 h. Under these conditions, both JDP2 and ATF3

proteins are present at detectable levels (Supplementary Fig. 1B). Four hours following the addition of TSA, ATF3 transcription was significantly induced by twenty fold (Fig. 9B). Conversely, the addition of TSA to serum-induced DKO MEF cells resulted in a significantly lower induction of ATF3 transcription as compared to wild type MEF cells (approximately 40% of wild type) (Fig. 9B). Consistent with the previous result, no difference is observed between WT and DKO cells following TSA treatment for CHOP10 and c-Jun transcripts. The significant elevation of ATF3 mRNA level in MEF cells treated with TSA also reflects the increase in ATF3 protein levels (Fig. 9C, top panel). Interestingly, no activation in c-Jun N-terminal kinase activity was observed under these conditions (Fig. 9C, middle panel), excluding the possibility that the potentiation of ATF3 transcription is due to a cellular stress response [3]. Importantly, similar expression level of various HDACs is observed in WT and DKO MEF cells (Supplementary Fig. 1C). Collectively, these results indicate that the ATF3 promoter is highly affected by HDAC activity during the 4 h serum induction and strongly highlight the contribution of JDP2 and ATF3 to the recruitment of HDAC activity to the ATF3 promoter.

JDP2 and ATF3 repress ATF3 transcription through the association with a CRE and a noncanonical ATF/CRE element located within the ATF3 proximal promoter at positions −90 and −20, respectively [15,16].

A

B
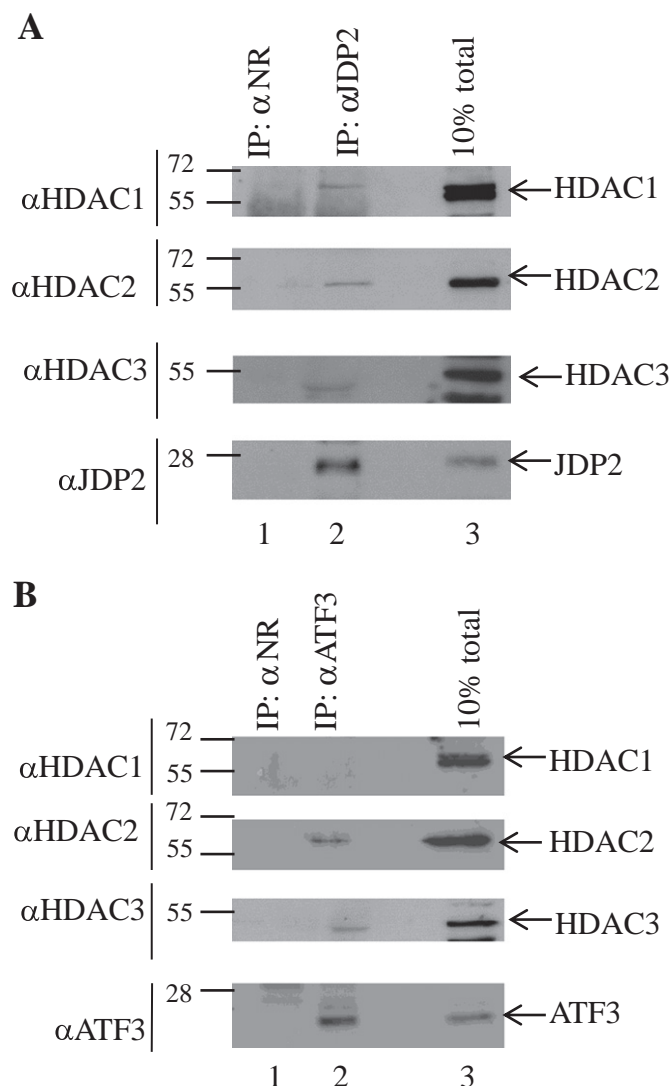
Fig. 6. Endogenous interaction of JDP2 and ATF3 with Class I HDACs. A. Serum starved MEF cell (0.5%) nuclear lysate was subjected to immunoprecipitation with either a non-relevant antibody (pre-immune serum, αNR lane 1) or anti-JDP2 antibody (αJDP2 lane 2) followed by Western blotting with the corresponding antibodies: anti-HDAC1, anti-HDAC2 and anti-HDAC3 (upper panels) or anti-JDP2 (lower panel). Lane 3 represents 10% of total cell lysate. B. Nuclear cell lysate was prepared from MEF cells that were induced with 20% serum for 1 h. Subsequently, lysate was subjected to immunoprecipitation with either a non-relevant antibody (pre-immune serum, αNR lane 1) or anti-ATF3 antibody (αATF3 lane 2) followed by Western blotting with the corresponding antibodies: anti-HDAC1, anti-HDAC2 and anti-HDAC3 (upper panels) or anti-ATF3 (lower panel). Lane 3 represents 10% of total cell lysate. Protein molecular weight markers (in kDa) are indicated on the left-hand side.

To examine the acetylated state of histones along the ATF3 promoter in wild type MEF cells as compared to DKO MEF cells, we used chromatin immunoprecipitation (ChIP) with anti-acetylated histone 4 and followed the histone acetylation state along the ATF3 promoter (Fig. 10A). Notably, the basal acetylation state within the proximal ATF3 promoter was generally higher in the DKO MEF cells (Supplementary Fig. 3B). Histone 4 acetylation was significantly induced by 2–5 fold along the promoter in wild type MEF cells (Fig. 10B). In contrast, the response to TSA treatment (histone 4 acetylation ratio) in DKO MEF cells was highly attenuated at three positions within the ATF3 promoter; at positions −1538 to −1388, −1134–1262 and −410 to −268. This data strongly suggests that JDP2 and ATF3 are responsible for the regulation

of histone 4 acetylation associated with the ATF3 promoter region located within a 1500 bp proximal to their DNA binding sites.

4. Discussion

The bZIP repressor proteins, JDP2 and ATF3, share a high degree of homology in their bZIP domains [3]. We have previously shown that both proteins have common target genes and also associate with similar proteins [7,16]. Here, we have identified HDAC6 as a common associating protein of both bZIP repressor proteins using the Ras recruitment system. It is possible that the classical two hybrid system is not ideal for the identification of HDAC interactions with transcription factors due to its transcription readout nature [22]. Thus, the use of a genetic system with a non-transcriptional readout, such as the Ras recruitment system, offers a great advantage for the identification of protein–protein interactions.

We mapped the association domain within HDAC6 to a 131 a.a. region in the C-terminus and to a 50 a.a. region within JDP2 consisting of the basic domain and three heptad leucine repeats. The three heptads fail to dimerize, suggesting that JDP2 dimerization is not required for the association with HDAC6. However, it is likely that protein dimerization accommodates the association with HDACs to form a trio-protein repressor complex. Such a protein complex was previously reported for JDP2 and HDAC3 [13]. As for ATF3, the minimal HDAC binding domain was mapped to the N-terminal and basic domain which does not include the leucine zipper domain, yet, the ATF3 full length protein displayed the strongest association with HDAC6. Previous studies described the overexpression of an ATF3 peptide corresponding to a.a. 1–100 resulting in potentiation of transcription of ATF3 target genes [6]. It was assumed that this domain competes with ATF3 for an inhibitory protein and therefore relieves the inhibitory effect. Yet, a possible inhibitory factor was not identified. Since the association of the ATF3 fragment 1–108 with HDAC6 is relatively significant, it is proposed that the putative inhibitory factor that is being titrated corresponds to various HDAC proteins.

Similarly, an inhibitory histone acetylase (INHAT) was described for JDP2. This domain directly associates with histones to compete for acetylation by p300 and ATF2 [12]. It is possible that HDAC association with histones increases the overall binding avidity of JDP2 to histones acting in concert to provide gene repression specificity.

Here, we also describe the association of ATF3 and JDP2 with HDACs 1, 2, 3, 5, 6 and 10. HDAC4, which is not expressed in somatic cells, associates very poorly with the bZIP repressors [34]. To the best to our knowledge the broad association with various HDAC members is a unique feature of ATF3 and JDP2. Multiple HDACs are found in stable complex with co-repressors such as Sin3, NuRD and co-REST [35]. The bZIP repressors may take part in these large complexes or form independent complexes. Both JDP2 and ATF3 proteins directly associate with HDAC6 and HDAC3 and do not require additional proteins for binding.

Previously, it was suggested that JDP2 indirectly associates with HDAC3 [13]. In that study, a GST pull-down was used to precipitate *in vitro* translated ³⁵S-labeled proteins that were pre-incubated for one h at 4 °C [13]. In our study, we observed that the interaction between bacterially purified JDP2 and HDAC3 was highly dependent on the incubation temperature. The physiological temperature (37 °C) may provide a thermodynamic flexibility to the N-terminal part of the leucine zipper motif to favor direct association with the bacterially purified HDACs 3 and 6.

The domain within the Class I HDACs 1 and 3 responsible for bZIP repressor binding is the DAC domain (Fig. 7). This domain displays a relatively high degree of homology (85%) between Class I members. The DAC domain of Class II HDACs displays much lower conservation with the Class I DAC domain [36]. Indeed, the binding of the bZIP repressors to HDAC6 is mapped to the unique BUZ C-terminal domain. This domain consists of a conserved zinc finger containing domain
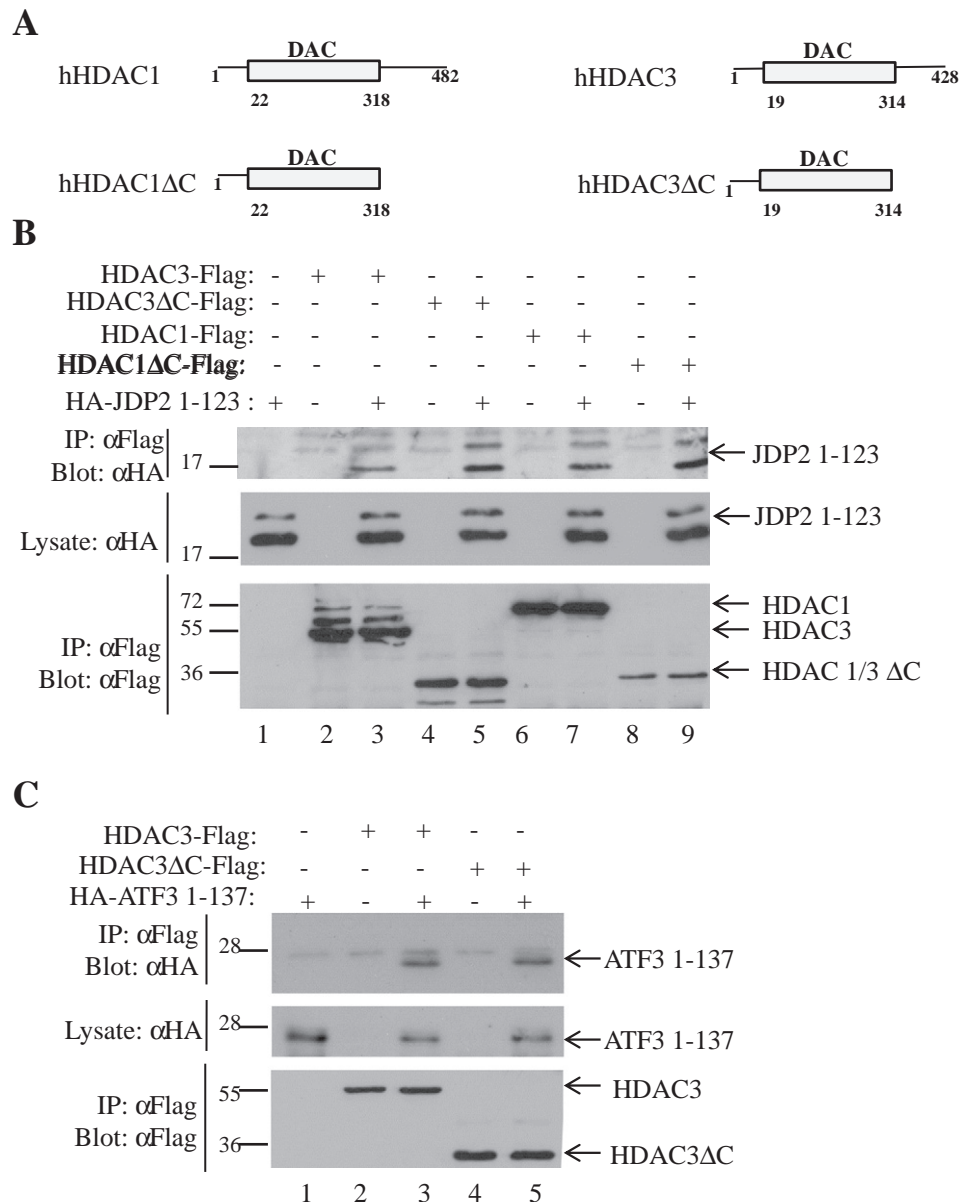
Fig. 7. Class I HDACs associate with JDP2 and ATF3 *via* the DAC domain. A. Schematic representation of the HDAC1 and HDAC3 full length and the C-terminal truncation constructs used in the experiments. B. HEK-293T cells were transfected with the HA-JDP2 fragment 1–123 (Fig. 3A) and HDAC1/3 Flag tagged corresponding to either full length or C-terminal deletion mutants in the combinations as indicated. Cell lysates were subjected to immunoprecipitation with anti-Flag antibodies followed by Western blotting with either anti-HA or anti-Flag (upper panel and lower panel, respectively). The expression level of the HA-JDP2 fragment was determined by blotting 10% of total cell lysate with an anti-HA antibody (middle panel). C. HEK-293T cells were transfected with HA-ATF3 fragment 1–137 (Fig. 4B) and HDAC3 Flag tagged corresponding to either full length or C-terminal deletion mutant in the combinations as indicated. Cell lysates were subjected to immunoprecipitation with anti-Flag antibodies followed by Western blotting with either anti-HA or anti-Flag antibodies (upper panel and lower panel, respectively). The expression level of the HA-ATF3 fragment was determined by blotting 10% of total cell lysate with an anti-HA antibody (middle panel). Protein molecular weight markers (in kDa) are indicated on the left-hand side.

shown to associate with ubiquitin monomers [41] mediating the regulation of polyubiquitin chain turnover [42]. In addition, the human HDAC6 harbors a cytoplasmic retention signal. Using biochemical fractionation, we failed to detect the translocation of either the endogenous JDP2 (Supplemental Fig. 4A) or ATF3 (Supplemental Fig. 4B) proteins to the cytoplasm as a result of human HDAC6 overexpression. Further studies are currently being conducted to determine the non-histone acetylation role of HDAC6 association with JDP2 and ATF3.

The ATF3 promoter displays a strong sensitivity to HDAC inhibition by TSA. A recent publication also suggested the elevation of ATF3 expression in human derived cancer cell lines following cellular treatment with histone deacetylase inhibitor-M344 [43]. In their study, it was suggested that the elevated ATF3 mRNA is not due to histone acetylation at the proximal ATF3 promoter. However, since ATF3

transcription is potentially regulated *via* alternate promoters [44], the interpretation of this analysis needs to be re-examined. ATF3 is needed to maintain homeostasis under stress conditions and therefore its expression is very tightly controlled [14,45]. Several mechanisms exist to maintain low basal expression level of ATF3 in exponentially growing cells under non-stressed conditions. These include transcriptional and post-transcriptional mechanisms. It appears that ATF3 auto-repression and recruitment of HDACs to the promoter by both ATF3 and JDP2 play a significant role in constitutive repression and the rapid shut-off of ATF3 expression following its induction.

In summary, we have shown that the homologous bZIP repressor proteins, ATF3 and JDP2, associate with multiple members of Class I and Class II HDAC family. Association occurs *via* the N-terminal domain independent of the leucine zipper dimerization interface. Here we have
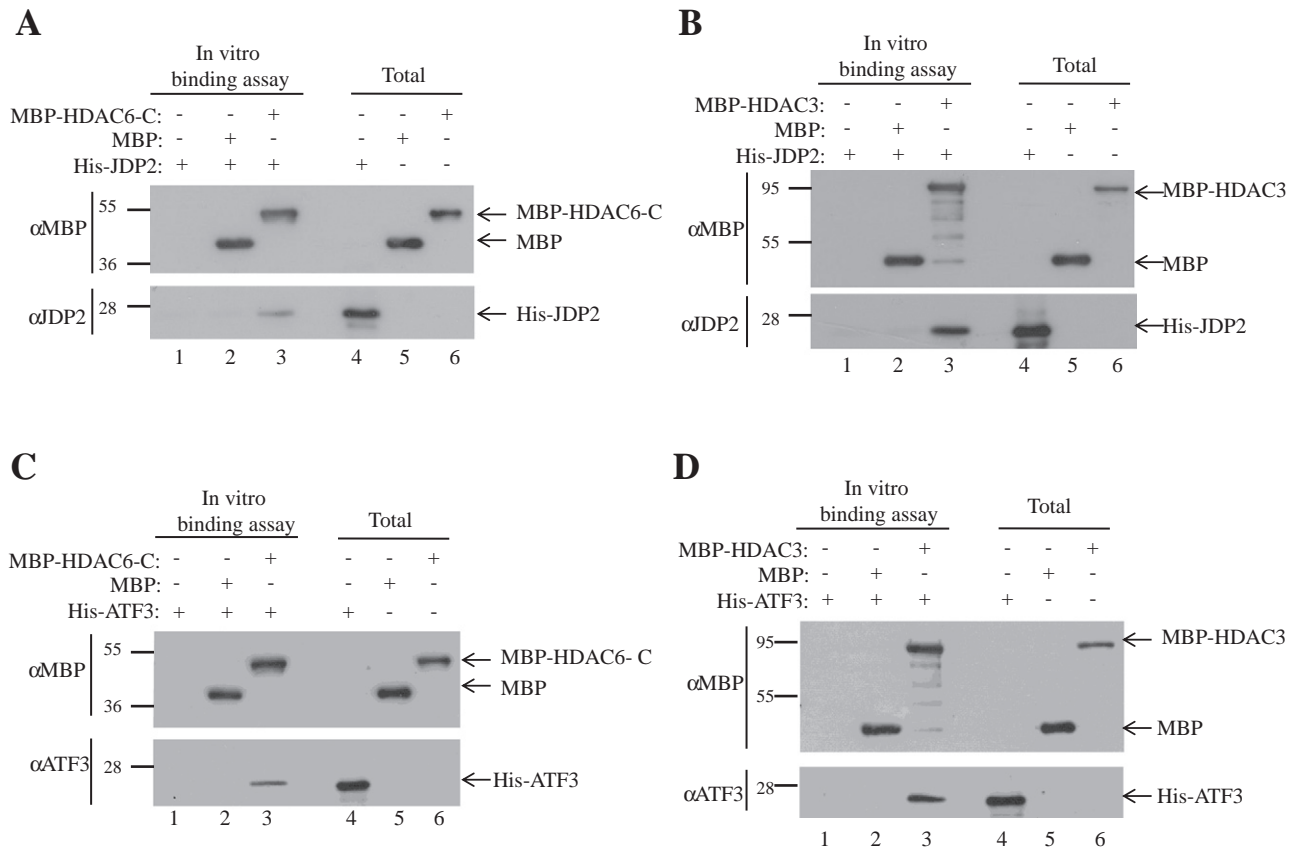
Fig. 8. The interaction between the bZIP repressors, JDP2 and ATF3, with HDAC6 and HDAC3 is direct. A–B. Bacterially purified His-JDP2, MBP and MBP-HDAC6-C (A) or MBP-HDAC3 (B) proteins (15 μg) were mixed for 2 h at 37 °C. Subsequently, protein complexes attached to amylose–sepharose beads were washed extensively and then eluted by maltose. Western blot analysis was performed with either anti-MBP (upper panels) or anti-JDP2 (lower panels) antibodies. Lanes 4–6 represent the corresponding purified proteins (0.5 μg). C–D. Bacterially purified His-ATF3, MBP and MBP-HDAC6-C (C) or MBP-HDAC3 (D) were subjected to an *in vitro* binding assay as described in A–B, followed by Western blotting with either anti-MBP (upper panels) or anti-ATF3 (lower panels) antibodies. Lanes 4–6 represent the corresponding purified proteins (0.5 μg). Protein molecular weight markers (in kDa) are indicated on the left-hand side.

also shown that the ATF3 promoter is subjected to constant acetylation/deacetylation modifications and HDACs play a significant role in the maintenance of ATF3's low basal level in the cells. Collectively, our results demonstrate that ATF3 and JDP2 are involved in recruiting HDACs to the ATF3 promoter region resulting in transcriptional repression of ATF3.

Acknowledgement

Appendix A. Supplementary data

Supplementary data to this article can be found online at http://dx.doi.org/10.1016/j.bbagrm.2012.09.005.

References

[1] Y.C. Huang, H. Hasegawa, S.W. Wang, C.C. Ku, Y.C. Lin, S.S. Chiou, M.F. Hou, D.C. Wu, E.M. Tsai, S. Saito, N. Yamaguchi, K.K. Yokoyama, Jun dimerization protein 2 controls senescence and differentiation *via* regulating histone modification, J. Biomed. Biotechnol. 2011 (2011) 569034.

[2] A. Aronheim, E. Zandi, H. Hennemann, S. Elledge, M. Karin, Isolation of an AP-1 repressor by a novel method for detecting protein–protein interactions, Mol. Cell. Biol. 17 (1997) 3094–3102.

[3] T. Hai, C.D. Wolfgang, D.K. Marsee, A.E. Allen, U. Sivaprasad, ATF3 and stress responses, Gene Expr. 7 (1999) 321–335.

[4] B.P.C. Chen, C.D. Wolfgang, T. Hai, Analysis of ATF3, a transcription factor induced by physiological stresses and modulated by gadd153/Chop, Mol. Cell. Biol. 16 (1996) 1157–1168.

[5] J.C. Hsu, R. Bravo, R. Taub, Interactions among LRF-1, JunB, c-Jun, and c-Fos define a regulatory program in the G1 phase of liver regeneration, Mol. Cell. Biol. 12 (1992) 4654–4665.

[6] B.P. Chen, G. Liang, J. Whelan, T. Hai, ATF3 and ATF3 delta zip. Transcriptional repression *versus* activation by alternatively spliced isoforms, J. Biol. Chem. 269 (1994) 15819–15826.

[7] K. Weidenfeld-Baranboim, K. Bitton-Worms, A. Aronheim, TRE-dependent transcription activation by JDP2-CHOP10 association, Nucleic Acids Res. 36 (2008) 3608–3619.

[8] S.E. Wardell, V. Boonyaratanakornkit, J.S. Adelman, A. Aronheim, D.P. Edwards, Jun dimerization protein 2 functions as a progesterone receptor N-terminal domain coactivator, Mol. Cell. Biol. 22 (2002) 5451–5466.

[9] C. Jin, H. Ugai, J. Song, T. Murata, F. Nili, K. Sun, M. Horikoshi, K.K. Yokoyama, Identification of mouse Jun dimerization protein 2 as a novel repressor of ATF-2, FEBS Lett. 489 (2001) 34–41.

[10] S. Katz, A. Aronheim, Differential targeting of the stress mitogen-activated protein kinases to the c-Jun dimerization protein 2, Biochem. J. 368 (2002) 939–945.

[11] S. Katz, R. Heinrich, A. Aronheim, The AP-1 repressor, JDP2, is a bona fide substrate for the c-Jun N-terminal kinase, FEBS Lett. 506 (2001) 196–200.

[12] C. Jin, K. Kato, T. Chimura, T. Yamasaki, K. Nakade, T. Murata, H. Li, J. Pan, M. Zhao, K. Sun, R. Chiu, T. Ito, K. Nagata, M. Horikoshi, K.K. Yokoyama, Regulation of histone acetylation and nucleosome assembly by transcription factor JDP2, Nat. Struct. Mol. Biol. 13 (2006) 331–338.

[13] C. Jin, H. Li, T. Murata, K. Sun, M. Horikoshi, R. Chiu, K.K. Yokoyama, JDP2, a repressor of AP-1, recruits a histone deacetylase 3 complex to inhibit the retinoic acid-induced differentiation of F9 cells, Mol. Cell. Biol. 22 (2002) 4815–4826.

[14] T. Hai, C.C. Wolford, Y.S. Chang, ATF3, a hub of the cellular adaptive-response network, in the pathogenesis of diseases: is modulation of inflammation a unifying component? Gene Expr. 15 (2010) 1–11.
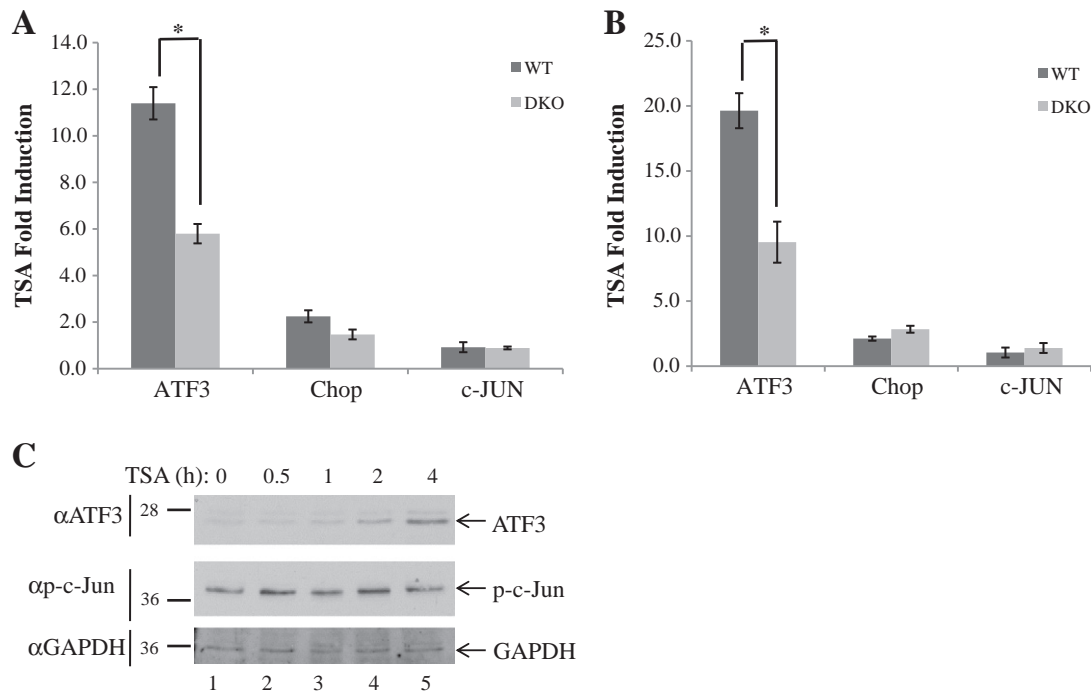
Fig. 9. Reduced sensitivity to HDAC inhibitor of the ATF3 promoter in JDP2 and ATF3 DKO MEF cells. A. mRNA was extracted from exponentially growing MEF WT and JDP2–ATF3 DKO cells in the presence or absence of 100 nM TSA for 4 h. qRT-PCR was used to determine the ATF3, Chop, c-Jun and GAPDH mRNA levels. The results represent the relative level of mRNA in cells treated with TSA as compared with untreated cells normalized with GAPDH. B. MEF WT and JDP2–ATF3 DKO cells were incubated in 0.1% serum 24 h before the induction by 20% serum in the absence or presence of 100 nM TSA for 4 h. Relative level of mRNA in cells with TSA as compared with cells treated with serum alone is shown. The expression level of ATF3, Chop and c-Jun is normalized with the expression of β2m. The results presented in A and B represent the mean and SEM of three (A) or four (B) independent experiments. *Asterisk* (*) indicates *P* value<0.01 when comparing WT and DKO. C. Western blot analysis with MEF nuclear extract cells treated at the indicated time with 100 nM TSA. The membrane was probed with anti-ATF3 (upper panel), anti-phospho-c-Jun (middle panel) and anti-GAPDH (lower panel). Protein molecular weight markers (in kDa) are indicated on the left-hand side.
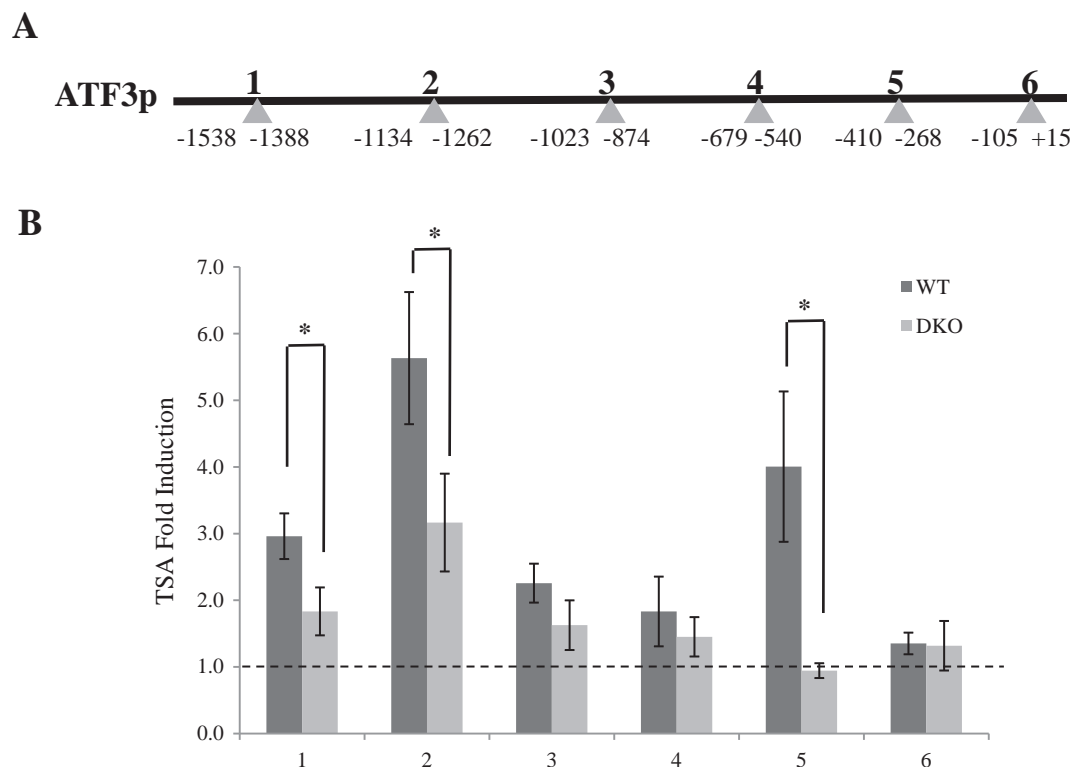
Fig. 10. Reduced histone 4 acetylation at the ATF3 promoter in JDP2 and ATF3 DKO MEF cells. A. Schematic representation of the ATF3 promoter and the location of the primers used relative to the transcription start site (+1). B. Chromatin immunoprecipitation using anti-acetylated histone 4 followed by qRT-PCR. The results represent the ratio of histone acetylation in the presence of TSA (3 h) at the indicated position within the ATF3 promoter (shown schematically in A). The dotted line represents ratio of one *i.e.* no alteration in acetylated histone 4 following TSA addition. The results represent the mean and SEM of three independent experiments. *Asterisk* (*) indicates *P* value<0.05 when comparing WT and DKO.

[15] C.D. Wolfgang, G. Liang, Y. Okamoto, A.E. Allen, T. Hai, Transcriptional autorepression of the stress-inducible gene ATF3, J. Biol. Chem. 275 (2000) 16865–16870.

[16] K. Weidenfeld-Baranboim, T. Hasin, I. Darlyuk, R. Heinrich, O. Elhanani, J. Pan, K.K. Yokoyama, A. Aronheim, The ubiquitously expressed bZIP inhibitor, JDP2, suppresses the transcription of its homologue immediate early gene counterpart, ATF3, Nucleic Acids Res. 37 (2009) 2194–2203.

[17] O. Ostrovsky, E. Bengal, A. Aronheim, Induction of terminal differentiation by the c-Jun dimerization protein JDP2 in C2 myoblasts and rhabdomyosarcoma cells, J. Biol. Chem. 277 (2002) 40043–40054.

[18] R. Heinrich, E. Livne, O. Ben-Izhak, A. Aronheim, The c-Jun dimerization protein 2 inhibits cell transformation and acts as a tumor suppressor gene, J. Biol. Chem. 279 (2004) 5708–5715.

[19] K. Bitton-Worms, E. Pikarsky, A. Aronheim, The AP-1 repressor protein, JDP2, potentiates hepatocellular carcinoma in mice, Mol. Cancer 9 (2010) 54.

[20] X. Yin, J.W. Dewille, T. Hai, A potential dichotomous role of ATF3, an adaptive-response gene, in cancer development, Oncogene 27 (2008) 2118–2127.

[21] S. Emiliani, W. Fischle, C. Van Lint, Y. Al-Abed, E. Verdin, Characterization of a human RPD3 ortholog, HDAC3, Proc. Natl. Acad. Sci. U. S. A. 95 (1998) 2795–2800.

[22] A. Aronheim, Ras signaling pathway for analysis of protein–protein interactions in yeast and mammalian cells, Methods Mol. Biol. 250 (2004) 251–262.

[23] J. Xu, Preparation, culture, and immortalization of mouse embryonic fibroblasts, Curr. Protoc. Mol. Biol. (2005) (Chapter 28, Unit 28.1.1–28.1.8).

[24] K. Nakade, J. Pan, A. Yoshiki, H. Ugai, M. Kimura, B. Liu, H. Li, Y. Obata, M. Iwama, S. Itohara, T. Murata, K.K. Yokoyama, JDP2 suppresses adipocyte differentiation by regulating histone acetylation, Cell Death Differ. 14 (2007) 1398–1405.

[25] M.G. Hartman, D. Lu, M.L. Kim, G.J. Kociba, T. Shukri, J. Buteau, X. Wang, W.L. Frankel, D. Guttridge, M. Prentki, S.T. Grey, D. Ron, T. Hai, Role for activating transcription factor 3 in stress-induced beta-cell apoptosis, Mol. Cell. Biol. 24 (2004) 5721–5732.

[26] G. Giaccone, J. Battey, A.F. Gazdar, H. Oie, M. Draoui, T.W. Moody, Neuromedin B is present in lung cancer cell lines, Cancer Res. 52 (1992) 2732s–2736s.

[27] J.P. Mather, Establishment and characterization of two distinct mouse testicular epithelial cell lines, Biol. Reprod. 23 (1980) 243–252.

[28] P. Batard, M. Jordan, F. Wurm, Transfer of high copy number plasmid into mammalian cells by calcium phosphate transfection, Gene 270 (2001) 61–68.

[29] K. Weidenfeld-Baranboim, L. Koren, A. Aronheim, Phosphorylation of JDP2 on threonine-148 by the c-Jun N-terminal kinase targets it for proteosomal degradation, Biochem. J. 436 (2011) 661–669.

[30] T. Hai, The ATF transcription factors in cellular adaptive responses, in: e. a Current Scientific Frontiers Book (Ma. J. (Ed.) In Gene Expression and Regulation, Higher Education Press, Beijing, China, and Springer, New York, USA, New York, 2006, pp. 329–340.

[31] Y.C. Broder, S. Katz, A. Aronheim, The Ras recruitment system, a novel approach to the study of protein–protein interactions, Curr. Biol. 8 (1998) 1121–1124.

[32] M. Hubsman, G. Yudkovsky, A. Aronheim, A novel approach for the identification of protein–protein interaction with integral membrane proteins, Nucleic Acids Res. 29 (2001) e18.

[33] S.S. Hook, A. Orian, S.M. Cowley, R.N. Eisenman, Histone deacetylase 6 binds polyubiquitin through its zinc finger (PAZ domain) and copurifies with deubiquitinating enzymes, Proc. Natl. Acad. Sci. U. S. A. 99 (2002) 13425–13430.

[34] A.J. de Ruijter, A.H. van Gennip, H.N. Caron, S. Kemp, A.B. van Kuilenburg, Histone deacetylases (HDACs): characterization of the classical HDAC family, Biochem. J. 370 (2003) 737–749.

[35] C.M. Grozinger, S.L. Schreiber, Deacetylase enzymes: biological functions and the use of small-molecule inhibitors, Chem. Biol. 9 (2002) 3–16.

[36] A. Clocchiatti, C. Florean, C. Brancolini, Class IIa HDACs: from important roles in differentiation to possible implications in tumourigenesis, J. Cell. Mol. Med. 15 (2011) 1833–1846.

[37] A. Aronheim, Y.C. Broder, A. Cohen, A. Fritsch, B. Belisle, A. Abo, Chp, a homologue of the GTPase Cdc42, activates the JNK pathway and is implicated in reorganizing the actin cytoskeleton, Curr. Biol. 8 (1998) 1125–1128.

[38] E. Shaulian, M. Karin, AP-1 as a regulator of cell life and death, Nat. Cell Biol. 4 (2002) E131–E136.

[39] H.F. Li, C.F. Cheng, W.J. Liao, H. Lin, R.B. Yang, ATF3-mediated epigenetic regulation protects against acute kidney injury, J. Am. Soc. Nephrol. 21 (2010) 1003–1013.

[40] Y. Cherasse, C. Chaveroux, C. Jousse, A.C. Maurin, V. Carraro, L. Parry, P. Fafournoux, A. Bruhat, Role of the repressor JDP2 in the amino acid-regulated transcription of CHOP, FEBS Lett. 582 (2008) 1537–1541.

[41] D. Seigneurin-Berny, A. Verdel, S. Curtet, C. Lemercier, J. Garin, S. Rousseaux, S. Khochbin, Identification of components of the murine histone deacetylase 6 complex: link between acetylation and ubiquitination signaling pathways, Mol. Cell. Biol. 21 (2001) 8035–8044.

[42] C. Boyault, B. Gilquin, Y. Zhang, V. Rybin, E. Garman, W. Meyer-Klaucke, P. Matthias, C.W. Muller, S. Khochbin, HDAC6-p97/VCP controlled polyubiquitin chain turnover, EMBO J. 25 (2006) 3357–3366.

[43] C. St Germain, A. O'Brien, J. Dimitroulakos, Activating transcription factor 3 regulates in part the enhanced tumour cell cytotoxicity of the histone deacetylase inhibitor M344 and cisplatin in combination, Cancer Cell Int. 10 (2010) 32.

[44] K. Miyazaki, S. Inoue, K. Yamada, M. Watanabe, Q. Liu, T. Watanabe, M.T. Adachi, Y. Tanaka, S. Kitajima, Differential usage of alternate promoters of the human stress response gene ATF3 in stress response and cancer cells, Nucleic Acids Res. 37 (2009) 1438–1451.

[45] T. Hai, M.G. Hartman, The molecular biology and nomenclature of the activating transcription factor/cAMP responsive element binding family of transcription factors: activating transcription factor proteins and homeostasis, Gene 273 (2001) 1–11.